HHS Public Access

Author manuscript

Int J Hyperthermia. Author manuscript; available in PMC 2021 December 22.

Published in final edited form as:

Int J Hyperthermia. 2020 ; 37(1): 696–710. doi:10.1080/02656736.2020.1778800.

Exosomes released by breast cancer cells under mild hyperthermic stress possess immunogenic potential and modulate polarization *in vitro* in macrophages

Kacoli Sen[1], **Austin E. F. Sheppe**[2], **Ishita Singh**[1], **Winnie W. Hui**[2], **Mariola J. Edelmann**[2], **Carlos Rinaldi**[1,3,*]

[1]Department of Chemical Engineering, University of Florida, Gainesville, USA

[2]Department of Microbiology and Cell Science, University of Florida, Gainesville, USA

[3]J. Crayton Pruitt Family Department of Biomedical Engineering, University of Florida, Gainesville, USA.

Abstract

Macrophages play a dual role in tumor initiation and progression, with both tumor-promoting and tumor-suppressive effects; hence, it is essential to understand the distinct responses of macrophages to tumor progression and therapy. Mild hyperthermia has gained importance as a therapeutic regimen against cancer due to its immunogenic nature, efficacy, and potential synergy with other therapies, yet the response of macrophages to molecular signals from hyperthermic cancer cells has not yet been clearly defined. Due to limited response rate of breast cancer to conventional therapeutics the development, and understanding of alternative therapies like hyperthermia is pertinent. In order to determine conditions corresponding to mild thermal dose, cytotoxicity of different hyperthermic temperatures and treatment durations were tested in normal murine macrophages and breast cancer cell lines. Examination of exosome release in hyperthermia-treated cancer cells revealed enhanced efflux and a larger size of exosomes released under hyperthermic stress. Exposure of naïve murine macrophages to exosomes released from 4T1 and EMT-6 cells post-hyperthermia treatment, led to an increased expression of specific macrophage activation markers. Further, exosomes released by hyperthermia-treated cancer cells had increased content of heat shock protein 70 (Hsp70). Together, these results suggest a potential immunogenic role for exosomes released from cancer cells treated with mild hyperthermia.

Keywords

Hyperthermia; macrophages; exosome; breast cancer; immune system

[*]**Corresponding Author Phone Number:** (352) 392-0881, **Fax Number:** (352) 392-9513, carlos.rinaldi@ufl.edu.

Conflict of interest:
The authors declare no conflict of interest.

1. Introduction

Thermal therapy involves temperature elevation of the whole body or a localized region, in order to achieve a therapeutic effect. Cancer treatment through local tumor thermal treatment involves utilization of high temperatures (>60°C) for ablation or febrile (41-43°C) or higher temperatures (45-47°C) for hyperthermia, as an independent therapy or in combination with chemotherapy or radiation therapy to yield enhanced therapeutic outcomes (Jeong 2014, Toraya-Brown and Fiering 2014, Seifert, Budach et al. 2016, Ha, Le et al. 2019, Phung, Nguyen et al. 2019). Hyperthermia has been described as primary or adjuvant-based therapy for cancer (Toraya-Brown and Fiering 2014). Recent advances in hyperthermia treatment regimens have focused on disease alleviation and the potential to enhance cancer therapeutics (Bettaieb, K et al. 2013). However, it has become apparent that hyperthermia causes activation of the immune system against cancer cells (Skitzki, Repasky et al. 2009, Yagawa, Tanigawa et al. 2017, Shao, O'Flanagan et al. 2019), resulting in great interest to improve understanding of the underlying mechanisms of this treatment.

Macrophages are an integral part of the immune system, playing a significant part in eliciting immune responses since they work in concert with downstream T cells (naïve or cytotoxic T cells) (Pozzi, Maciaszek et al. 2005, Ley 2014). Macrophages play a dual role in tumor initiation and progression and are known to have both tumor-promoting and tumor-suppressive effects (Poh and Ernst 2018). However, the response of macrophages to cells that have been exposed to a hyperthermic environment has not yet been clearly defined.

Breast cancer includes cancers of the cells associated with the lobules or ducts of the breast. Breast cancer is the most commonly diagnosed type of cancer in women in the United States of America (Siegel, Miller et al. 2019). Screening efforts, such as clinical breast exams and mammograms or onset of clinical symptoms, lead to a breast cancer diagnosis. Even though drug discovery endeavors focused on breast cancer have yielded a wide array of chemo-therapeutics, including taxanes, cyclophosphamide, carboplatin, capecitabine, and 5-fluorouracil, lack of drug sensitivity and development of resistance demands the development of combinatorial or adjuvant therapies (Gonzalez-Angulo, Morales-Vasquez et al. 2007, Moreno-Aspitia and Perez 2009, Selli and Sims 2019). Exploring alternative therapeutic modalities such as hyperthermia could lead to treatments that overcome the limiting factors of classical therapeutics in breast cancer treatment.

Cells constitutively secrete endosome-derived, nano-sized extracellular vesicles (60-120 nm) known as exosomes, which act as functional vehicles carrying a complex cargo with messenger molecules in the form of proteins, lipids, and nucleic acids (Théry, Amigorena et al. 2006, Beninson and Fleshner 2014, Rezaie, Ajezi et al. 2017, Zhang, Liu et al. 2019). Physiological challenges like injury, inflammation, infection, disease (Beninson and Fleshner 2014), or application of exogenous stress like heat (Chen, Guo et al. 2011) or irradiation (Ratajczak, Wysoczynski et al. 2006) can alter genetic or proteomic content of exosomes, as well as their function. The role of stress-modified exosomal cargo as an immunogenic mediator may be an attractive platform for activating an anti-tumor immunogenic effect.

The focus of the present study was to assess the effect of hyperthermia on exosome release by cancer cells and evaluate the effect of exosomes released by heat-treated cancer cells on the polarization of naïve macrophages. Experiments demonstrate increased exosome secretion and increased exosome size for cancer cells treated with mild hyperthermia. In this study stimulation of the RAW 264.7 murine macrophage cell line by exosomes derived from EMT-6 and 4T1 murine breast cancer cell lines were evaluated. Exosomes from breast cancer cells under hyperthermic stress were found to activate macrophages with the release of cytokines, which may alter adaptive immune response. These studies suggest a potential immunogenic role of exosomes released by hyperthermia treated cancer cells.

2. Materials and Methods

2.1. Materials

3-(4, 5-dimethyl-2-thiazolyl)-2, 5-diphenyl-2H-tetrazolium bromide (MTT), NP-40 Cell Lysis Buffer (IGEPAL CA-630), glutaraldehyde, phosphate-buffered saline (PBS), Waymouth's MB 7521 medium, Lipopolysaccharides (LPS) from *Escherichia coli* O26: B6 were all purchased from Sigma Chemicals Co., USA. Alexa Fluor 488 Phalloidin and Micro BCA Protein Assay were obtained from Thermo Fisher Scientific, USA. Dulbecco's modified Eagle's medium (DMEM), Roswell Park Memorial Institute 1640 medium (RPMI-1640), and their supplementations of fetal bovine serum (FBS), penicillin, and streptomycin were all procured from Gibco (Invitrogen), USA. ExoAb Antibody Kit containing CD9, CD63, CD81, Heat Shock Protein 70 (Hsp70) primary antibodies were acquired from Systems Biosciences, USA, while IRDye 800CW Donkey anti-Rabbit IgG secondary antibody was obtained from LI-COR, USA. Ammonium molybdate tetrahydrate was procured from EMD Millipore, USA while Protease Inhibitor Cocktail was purchased from Roche, USA. ELISA kits against Interleukin 10 (IL-10), Regulated upon Activation, Normal T cell Expressed, and Secreted (RANTES), Tumor Necrosis Factor α (TNF α) were acquired from RayBiotech, USA. All other chemicals used were of the highest analytical grade available. The chemicals were used as obtained without further purification. Ultrapure water obtained from Synergy Water Purification System (EMD Millipore, USA) was used for all experiments.

2.2. Methods

2.2.1. Cell culture conditions—Murine breast cancer cells EMT-6 and 4T1 and murine macrophage cell line RAW 264.7 were obtained from the American Type Culture Collection, USA, and grown as adherent cultures in 10%−15% heat-inactivated, FBS supplemented Waymouth, RPMI-1640, and DMEM medium respectively at 37°C in a 5% CO_2 and 95% humidified conditions. After the cells reached 80% confluence, they were trypsinized (0.25% Trypsin and 0.1% EDTA) or scrapped, centrifuged (Eppendorf, Germany), and suspended in the appropriate medium respectively. Cells used for this study were mycoplasma free, obtained from passage numbers <20, and displayed ≥ 95% viability (Trypan Blue assay). For subsequent experiments, the cells were seeded in sterile 96-well plates (with 8-well strips), transwells, chambered slides, and 100-mm culture plates, as required.

The primary bone marrow-derived macrophages (BMDMs) used in this study were isolated and cultured as previously described (Amend, Valkenburg et al. 2016, Hui, Hercik et al. 2018). The BMDMs were isolated from bone marrow flushed from the femurs and tibias of BALB/c mice maintained and euthanized in accordance with institutional guidelines. The isolated BMDM were cultured in RPMI 1640 medium supplemented with 10% heat-inactivated FBS, 100 U/ml penicillin, and 100 μg/ml streptomycin. In order to obtain differentiated macrophages, macrophage colony-stimulating factor (5 ng/ml) was added every 2 days for a week along with fresh media. After a week, the differentiated macrophages were detached by adding ice-cold PBS followed by incubation at 4°C for 10 minutes. The macrophages were detached by gently pipetting the PBS of the plates, followed by centrifugation at 200 × g for 5 minutes. For subsequent experiments, the cells were counted, resuspended in sterile BMDM cultivation media and seeded in sterile 24-well plates.

2.2.2. Thermal dose determination—In hyperthermia treatment, the extent of cell death or level of inhibition is dependent on the temperature and exposure time, and hence, a method to normalize the various time-temperature regimens is essential. The dose metric called Cumulative Equivalent Minutes at 43°C (CEM43) which reflects the heat-based inhibitory or cytotoxic effect elicited by heat exposure at 43°C was utilized in this study. The concept of CEM43 was first demonstrated and proposed by Sapareto and Dewey in 1984 as a normalizing method to convert different thermal doses (different time-temperature exposures) to equivalent exposure times at a reference temperature of 43°C (Sapareto and Dewey 1984, van Rhoon, Samaras et al. 2013) and involves using the equation:

$$\mathrm{CEM43^{\circ}C} = \sum_{i=1}^{n} t_i \cdot R^{43-Ti} \quad (1)$$

where CEM43°C is the Cumulative Equivalent Minutes at 43°C, t_i is the i-th time interval, R is variable related to the temperature dependence of the rate of cell death (R=0.25 when T<43 °C, R= 0.5 when T>43 °C), and T is the exposure temperature during time interval t_i. The Cumulative Equivalent Minutes at 43°C Thermal $Dose_{50}$ (CEM43 TD_{50}) described in this study is reflective of the treatment time at which 50% of the test sample was inhibited at 41-45°C respectively, converted to equivalent thermal dose at 43°C.

2.2.3. Cell viability assay—The murine cell lines EMT-6, 4T1, and RAW 264.7 were harvested in the exponential growth phase and seeded in sterile 96-well flat-bottom culture plates (with 8-well strips) at an optimized concentration of 2×10^3 cells per well in 100μl of FBS-supplemented Waymouth or RPMI-1640 or DMEM medium respectively. Cells were incubated overnight and then exposed to incubator based hyperthermia (41-45°C for 5-160 minutess). This procedure was followed by a recovery period equivalent to 2 doubling times (EMT-6 and RAW 264.7= 24 hours, 4T1=48 hours). These untreated or treated cells were either subjected to MTT assay or flow cytometric analysis following the Annexin V-FITC-PI assay.

For the MTT assay, the culture medium was removed, and 100μl of MTT dye dissolved in media (1mg/ml) was added to each well. After incubating for 5 hours, the unreduced

MTT solution was discarded, and 100 μl of DMSO was added to each well to dissolve the purple formazan precipitate. The plates were gently shaken, and the amount of formazan in solution was quantified by measuring the absorbance of the solution at 570nm (A_{570}) using a microplate reader (SpectraMax® M5, Molecular Devices, USA). The hyperthermia based cellular inhibition was expressed in terms of percent cell viability relative to untreated control cells, defined as:

$$\% \text{ Cell viability} = [(A_{570} \text{ treated cells}) / (A_{570} \text{ untreated control cells})] \times 100 \quad (2)$$

The inhibitory thermal dose that affected 50% of the test population was determined from three independent experiments.

For the Annexin V-FITC-PI assay, the cellular media of untreated or treated EMT-6, 4T1, and RAW 264.7 were collected 24 hours after treatment. The adherent cells were detached with trypsin and the cells were collected and combined with the original supernatant. The cells were resuspended in 1 mL 1X Annexin V binding buffer (Annexin V Binding Buffer, 10X concentrate) maintaining the cellular concentration at ~1×10^6 cells/ml. From this stock 200 μl was transferred (~2×10^5 cells) to a centrifuge tube. To the cell suspension, 10 μl of fluorochrome-conjugated Annexin V (eBioscience™ Annexin V Apoptosis Detection Kit FITC) was added and incubated for 10-15 minutes at room temperature in the dark. The cells were spun down at 300 × g for 10 mins. To each tube, 0.2 μl of PI (1mg/ml) in 100 μl final cell suspension was added and the tubes were incubated in the dark for 15 minutes at room temperature. The cells were then washed with 500 μl 1 × Annexin V binding buffer and spun down at 335 × g for 10 minutes. The cells were fixed with 3.7 % formaldehyde on ice for 10 minutes. Fixation was followed by washing with 1 x PBS and spin down at 425 × g for 8 minutes to decant the supernatant. The cell pellet was suspended in 100 μl of a 50 μg/ml stock of RNase (dissolved in 1X Annexin V binding buffer) and incubated for 15 min at 37°C to ensure that only DNA and no RNA is stained. The samples were then analyzed on FACS Canto II (BD Bioscience, USA) flow cytometer. A total of 10,000 events were acquired for each sample and data obtained were processed with the BD FACS Diva software package.

2.2.4. Isolation of exosomes—Exosomes derived from control or treated breast cancer cells were isolated by ultracentrifugation, as described previously with slight modifications (Théry, Amigorena et al. 2006, Hui, Hercik et al. 2018, Han, Zhou et al. 2019, Zheng, He et al. 2019). Briefly, serum free cell culture supernatants containing secreted extra-vesicular bodies were collected from cells with or without hyperthermia treatment and supplemented with phosphate-buffered saline containing protease inhibitor cocktail (Roche, USA). The cell culture supernatants were centrifuged first for 10 minutes at 300 × g, then 2,000 × g for 10 minutes followed by a final cycle at 10,000 × g for 30 minutes to remove cellular debris, apoptotic bodies, and microvesicles sequentially. Following the sequential centrifugation steps at 4°C, the supernatant was filtered using a 0.22 μm syringe filter and subjected to ultracentrifugation at 100,000 × g for 60 minutes at 4°C (T-890 Rotor, Thermo Scientific, USA). The exosome pellet was washed with cold PBS, followed by another round

of ultracentrifugation at 100,000 × g for 60 min at 4°C. The final exosome pellet was resuspended in sterile PBS containing 1X protease inhibitor cocktail.

2.2.5. Determination of exosome size distribution—A NanoSight LM10 (Malvern, UK) was used to characterize the isolated exosomes in terms of mean diameter and concentration (EV ml^{-1}). The appropriately diluted exosome samples were injected into the sample chamber of the instrument, and the particle size distribution was obtained through nanoparticle tracking analysis (NTA). The number of exosomes has been standardized to the final number of viable cells yielding the exosomes. PBS was analyzed as a negative control. The mean square displacement of the particles that cross the laser path was detected by the instrument, and the Stokes-Einstein equation was utilized to calculate the hydrodynamic diameter of the particles. Direct measurements of the particle distribution and concentration of particles per ml of sample were obtained by acquiring data of a large number of scattering trajectories over multiple runs.

2.2.6. Transmission Electron Microscopy (TEM)—The exosomes were fixed and embedded on copper EM grids with formvar coating stabilized by holey carbon film as described previously (Théry, Amigorena et al. 2006). The exosome pellet obtained after the last round of ultracentrifugation was resuspended and fixed in 50 μl of 2% paraformaldehyde (pH 7.4). A sample containing 10 μl of the fixed exosome isolate was deposited on the grid, and sufficient time was allowed for exosomes to adsorb onto the grid. Grids were washed gently with PBS, followed by secondary fixation with 1% glutaraldehyde for 5 min. The grids were washed to remove the glutaraldehyde, and the samples were contrast stained first with uranyl-oxalate at pH 7, for 5 min followed by a mixture of 4% uranyl acetate and 2% methylcellulose in a ratio of 100 μl/900 μl, which allowed secondary staining and embedding.

2.2.7. Scratch and Transwell migration assays—To test the migration eliciting effect of exosomes released post hyperthermia treatment from 4T1 and EMT-6 cells, 8-μm filter-fitted transwells were placed in a 24-well tissue culture sterile plate. RAW 264.7 cells (1×10^6) suspended in incomplete growth medium were added to the top chamber. The bottom well was filled with medium containing either LPS as a chemoattractant or 1×10^6 exosomes. After 24 h incubation at 37°C in a 5% CO_2 atmosphere, cells that migrated to the lower surface of filters were detected with crystal violet staining. Cells were counted under an inverted phase-contrast microscope and imaged under 20× bright field magnification for visual evidence.

To assess the invasiveness of cells in response to hyperthermia, 1×10^5 cells were seeded on a 6-well tissue culture plate and allowed to proliferate for 24 hours to obtain a confluent monolayer, and their migratory response was studied in control and treated set by *in vitro* wound or scratch assay. A wound was introduced in the cellular monolayer by creating a straight scratch with a 200 μl micropipette tip. Cellular debris were removed, and the scratch was imaged right away for time point 0 hour. Regions imaged on the plate were saved on the Keyence microscope (BZ-X700 Keyence, USA) using the multi-point capture feature to ensure that the same regions of the scratch were imaged after treatment. After 24 hours incubation, the distance between the adjacent free edges of the scratch was measured using

Image J software to estimate the invasiveness of the cells. Statistical analysis was performed to obtain p-values of wound width using paired t-test between the same treatment group, before and after treatment. Each experiment was performed in triplicate.

2.2.8. Scanning electron microscopy (SEM) study—SEM analysis was performed according to the protocol described elsewhere with slight modifications (Sen, Banerjee et al. 2019). RAW 264.7 cells were seeded at a density of 5×10^3 cells on sterile glass coverslips. The cells were untreated/treated with 1×10^6 exosomes or 100 ng LPS for 24 hours (positive control). The cells were washed three times with PBS (1X) and fixed with 2% glutaraldehyde in phosphate-buffered saline (pH 7.4) for 1 h at room temperature in the dark. The cells were again washed three times with PBS (1X) and dehydrated through a graded ethanol series (50, 70, 90, 95, and 100%). A drop of HMDS (1, 1, 1, 3, 3, 3-Hexamethyl disilazane) was added and left to air dry at room temperature. The cells were sputter-coated with gold and imaged with a scanning electron microscope (Hitachi SU5000 SEM, Japan) using an acceleration voltage of 20kV.

2.2.9. Cellular binding study—For the study of cellular binding of exosomes, the adhered RAW 264.7 cells (1×10^4 cells per chamber in an 8-well chambered slide) were incubated with Nile red-stained exosomes for 3, 6, 12, and 24 hours. To stain the exosomes, 1×10^6 vesicles (quantified using NTA) were incubated with the Nile red (3μg/ml) for 30 minutes, followed by 100,000 × g ultracentrifugation for 1 hour (two cycles to wash out free Nile Red). The treated/untreated cells were washed, fixed, permeabilized, stained for actin using Alexa Fluor™ 488 Phalloidin, mounted in DPX mounting medium, and imaged with a fluorescence microscope (BZ-X700 Keyence, USA).

2.2.10. Macrophage treatment with exosomes and ELISA—Murine macrophage RAW 264.7 cells were seeded at a density of 10^4 in each chamber of an 8 well-chambered slide, allowed to adhere overnight, and subsequently treated or left untreated. Treatment regimens were a) 100 ng LPS for 24 hours (positive control), b) untreated 4T1-derived exosomes, c) HT treated 4T1-derived exosomes, d) untreated EMT-6-derived exosomes, and e) HT treated EMT-6-derived exosomes. The exosome-treated sets of cells were exposed to 1×10^6 vesicles for 24 hours. The RAW 264.7 supernatant was collected for ELISA analysis of IL-10, TNF-α, and RANTES according to the manufacturer's instructions (RayBiotech, USA).

2.2.11. Western blot—Isolated exosomes were lysed using NP-40 Cell Lysis Buffer (IGEPAL® CA-630) supplemented with 1 mM phenylmethylsulfonyl fluoride (Sigma Chemicals Co., USA) and protease and phosphatase inhibitors (Roche, USA). Proteins were quantitated using the micro Bicinchoninic Acid (BCA) Protein Assay kit (ThermoFisher Scientific, USA) in a benchtop plate reader. Equivalent concentration of proteins or vesicles were then carefully loaded in each lane of a 12% polyacrylamide gel and electrophoresed appropriately. The proteins were meticulously transferred onto a nitrocellulose membrane (GE Healthcare Life Sciences, United Kingdom), and the blots were probed with appropriate primary antibodies followed by secondary antibodies at supplier's recommended dilutions.

Immunoblots were then imaged using Near-Infrared fluorescent detection and imaging systems (Odyssey® CLx Infrared Imaging, LI-COR, USA).

2.2.12. Transcript Analysis by RT-qPCR—The total RNA from untreated or exosome treated RAW 264.7 and BMDM cell lines was extracted using the Qiagen RNeasy Mini Plus extraction kit, followed by cDNA generation using the Verso cDNA synthesis kit (Thermo Fisher) with randomized hexamers. The expression of genes Arg-1 and iNOS were measured by using a two-step quantitative real-time polymerase chain reaction (RT-qPCR) which was performed using SYBRGreen reagents (Bio-Rad) on the Stratagene MXP3005. Gene expression was normalized to the expression of the housekeeping gene GAPDH and expressed as fold change estimated by using the ΔΔCt method, and the statistical significance was reported as previously described (Sheppe, Kummari et al. 2018). Primers used for the study are listed in Table 1 (melt curve in supplementary materials Figure S-1) and have been based on prior work (Zhou, Jiao et al. 2017).

2.2.13. Statistical Analysis—Prism 5 software (GraphPad Software, Inc., La Jolla, USA) was used for statistical analyses. Data are presented as mean ± S.D. values (n=3). The statistical significance or variance was determined by using paired or unpaired Student's t-test in experiments where control set values were reported and one-way analysis of variance (ANOVA) with Tukey's post-hoc test in case of tests where the variance between experimental (test) sets was assessed. *$p<0.05$ was considered statistically significant while ***$p<0.001$ was considered statistically highly significant.

3. Results and discussion

3.1. Determination of suitable hyperthermia thermal dose

The concept of CEM43 is translatable *in vitro* and also extrapolatable in patient groups with low variation in terms of tumor size and heterogeneity (van Rhoon 2016) and contributes highly to determine the prognostic ability and effectiveness of a thermal dose (time-temperature regimen) for a disease system. The Cumulative Equivalent Minutes at 43°C Thermal $Dose_{50}$ (CEM43 TD_{50}) described in this study is reflective of the treatment time at which 50% of the test sample was inhibited at 41-45°C respectively, converted to equivalent thermal dose at 43°C [Figures 1 (a, b), S-2, Table 2]. Using the CEM43 TD_{50}, allowed conversions across different temperature-time treatment regimens in murine cell lines EMT-6, 4T1, and RAW 264.7 (Table 2) while also providing a reference point for determining an equivalent treatment regimen for the different cell lines. The results of the MTT assay corroborated with that obtained by flow cytofluorimetric analysis as assessed by Annexin V-FITC-PI assay under conditions corresponding to CEM43 TD_{50} for both cell lines [Figure 1 (c, d) and Figure S-3]. In this study, the conditions corresponding to CEM43 TD_{50} was applied for all the subsequent experiments.

3.2. Hyperthermia treatment alters the yield and size distribution of exosomes released by cancer cells

A recent analysis of extracellular vesicles (< 150nm) has led to the reclassification of the secreted extracellular bodies into three different populations: exomeres (< 50 nm;

approximately 35 nm), small exosomes (Exo-S, size: 60-80 nm), and large exosomes (Exo-L; 90-120 nm). The molecular signatures of exomeres are distinct since they do not express tetraspanins and preferentially pack Hsp90, while exosomes (Exo-S/Exo-L) carry tetraspanins (CD9, CD63) and Hsp70 (Zhang, Freitas et al. 2018).

Comparative analysis of the size of exosomes derived from treated or untreated 4T1 and EMT6 cell lines suggests an increase in mean diameter in the hyperthermia treated groups. Figures 2, Figure S-4, S-5 and Table 3 show the exosome size distribution in untreated and hyperthermia treated cells. The average mean diameter for control untreated 4T1 and EMT-6 cells was 71.7 nm and 96.7 nm, respectively, while exosomes released after exposure to hyperthermic conditions had mean diameters of 118.6 nm and 140.3 nm, respectively. These observations suggest an increase in mean diameter due to heat-based stress. Under homeostatic conditions, the Exo-S: Exo-L ratio is high due to a more significant predominance of smaller sized population. However, under hyperthermic stress, the Exo-S: Exo-L ratio is reduced due to the greater abundance of Exo-L in the isolated fractions. Moreover, there was more heterogeneity in the size of exosomes released after hyperthermia.

Exosome isolates obtained from homeostatic cells were characterized by the presence of particles of uniform size, which yielded a single sharp peak, as observed in Figure S-4 (a, c) and Figure S-5 (a, b). Some exosome isolates from homeostatic cells yielded a sharp peak, with one or more relatively small peaks [Figures S-4 (b), S-5 (c)]. Importantly, all exosome samples isolated from cells post-hyperthermia showed multiple size peaks in a broad size range, as observed in Figure S-4 (d-f) and Figure S-5 (d-f).

When comparisons were made between control and treated experimental groups under identical seeding and isolation conditions, a statistically significant increase in the number of exosomes was observed in both cell lines [$p=0.0376$ for 4T1, $p=0.0174$ for EMT-6] [Figure 2(a), 2(c)]. This difference is reflective of cellular stress and may be attributed to efforts by the cell to ameliorate the condition by releasing stress signals as a part of cellular crosstalk.

3.3. Exosomes secreted by cancer cells post-hyperthermia treatment have altered morphology

Conventional TEM was used to visualize the morphology of 4T1-and EMT-6-derived exosomes. Cryo-TEM studies with exosomes yield a spherical shape since the technique involves visualization in the native state without the use of stains or fixatives (Sharma, LeClaire et al. 2018). However, in conventional TEM based imaging, large-sized exosomes (50-100nm) exhibit a central depression/pallor or cup-shaped morphology while smaller exosomes (~50 nm) do not display the central depression or cup-shaped morphology (Théry, Amigorena et al. 2006). The TEM analysis of negatively stained exosomes for both 4T1 and EMT-6 hyperthermia-derived exosomes (Figure 3) revealed a greater abundance of cup-shaped membrane vesicles than untreated sets from respective cell lines, which was in line with the NTA data where the mean diameter of the vesicles was higher for the hyperthermia treated than that of the control untreated sets (Table 3).

3.4. Breast cancer cells or macrophages post-hyperthermia treatment exhibit no change in wound healing behavior

A series of wound healing assays were performed on EMT-6, 4T1, and RAW 264.7 cells to assess their migratory potential under homeostatic conditions and hyperthermic stress. Cancer cells are intrinsically invasive and exhibit enhanced proliferation relative to normal healthy cells (Krakhmal, Zavyalova et al. 2015). Changes in wound size in 4T1 and EMT-6 cells were monitored, and it was observed that there was no significant change in wound recovery potential after hyperthermia treatment in both breast cancer cell lines [Table S (1-2), Figure S-6]. This data suggests that hyperthermia alone may not affect the invasiveness of the cancer cells.

The wound-healing assay was also performed on RAW 264.7 cells to determine if hyperthermic stress affected their migratory ability. For this study, the experimental conditions included untreated control, positive control (LPS), hyperthermia, and the combination of hyperthermia and LPS. LPS has been reported to be a chemoattractant for RAW 264.7 macrophages over a concentration gradient and induces migratory behavior by MMP10 regulation (Mummidi, Murray et al. 2013). Macrophages did not show rapid proliferative behavior in either treated or untreated groups [Figure S-7]. These results point out that macrophages under homeostatic conditions are dormant and are not activated to be motile under hyperthermic conditions in a pathologically disease-free state.

3.5. Exosomes secreted by cancer cells post-hyperthermia treatment increase macrophage migration

The migration of immune cells to tumor cells is a critical factor in initiating an immune-based anti-tumorigenic effect. The exchange of biochemical messages between cancer cells and immune cells of the body as a part of cellular cross-talk is necessary for an immune-based anti-neoplastic effect. Exosomes have been reported to be fundamental units of intercellular communication (De Toro, Herschlik et al. 2015, Mathieu, Martin-Jaular et al. 2019), but they also act as cellular stress messengers by packaging unique cargo depending on the cellular condition (de Jong, Verhaar et al. 2012, Vulpis, Soriani et al. 2019, Williams, Coimbra et al. 2019).

A set of transwell studies was designed for discerning the effect of tumor cell-derived exosomes on macrophage migration. Macrophages showed migratory behavior when they were stimulated by a concentration gradient of the chemoattractant LPS or exosomes released by 4T1 and EMT-6 cells after hyperthermic stress [Figure 4 (a, b)]. Exosomes released under homeostatic conditions from EMT-6 or 4T1 did not elicit migratory behavior from macrophages, suggesting that exosomes released by cancer cells subjected to hyperthermic stress contain signals mediating a migratory response in treated macrophages.

3.6. Exosomes secreted by cancer cells post-hyperthermia treatment alter macrophage morphology

SEM study of untreated control and exosome treated RAW 264.7 cells was performed to investigate the effect of the exosome isolates from 4T1 and EMT-6 on macrophage morphology. The positive control for this study involves stimulation and activation of

macrophages by LPS. Activated macrophages display a more flattened structure resulting in increased cytoplasmic protrusions, which happens during their activation and accelerated proliferation (Wu, Li et al. 2013).

Macrophages treated with exosomes from control untreated 4T1 and EMT-6 cells did not exhibit changes in morphology (Figure 5). However, macrophages treated with exosomes derived from hyperthermia-exposed EMT-6 or 4T1 cells exhibited a flattened appearance with increased cellular processes similar to that elicited by LPS (Figure 5, Figure S-8). Cellular binding of exosomes released from breast cancer cells 4T1 and EMT-6 was studied in RAW 264.7 cells, where Nile Red-stained exosomes were observed as red puncta around the cells after 3 and 6 hours of incubation (Figure S-9, S-10).

3.7. Exosomes from heat-treated cells induce a pro-inflammatory response in macrophages

Heat shock protein 70 (Hsp70) is a component of the intracellular heat shock protein family, which is expressed in both prokaryotes and eukaryotes (Ghazaei 2017). The heat shock proteins maintain cellular homeostasis and promote cell survival in response to temperature-induced stress while also playing a significant role in immune reactions. Previous studies have suggested that hyperthermia treatment of tumor cells leads to the expression of Hsp70, which can elicit host antitumor immunity (Ito, Shinkai et al. 2001, Ito, Matsuoka et al. 2003). In our study, we found that exosomes secreted by breast cancer cells in stress-induced (heat shock at 43°C at CEM TD_{50}) conditions had increased Hsp70 content. Specifically, exosomal Hsp70 was significantly increased after exposure to heat stress for murine breast cancer cell lines [p=0.0415, 0.0184 for EMT6 and 4T1, respectively] [Figure 6 (a, b)]. Since exosomal membranes are abundant in the endosome-specific tetraspanins (CD9 and CD63), these two proteins were also analyzed as exosomal markers [Figure 6 (c, d)].

Next, since Hsp70 is a modulator of tumor cell immunogenicity (Ito, Shinkai et al. 2001), we evaluated the downstream effect of Hsp70-containing exosomes derived from hyperthermia treated cancer cells on macrophages. Treatment with exosomes derived from hyperthermia-treated breast cancer murine cell lines led to TNF-α release in macrophages (Figure 7), suggesting an immunostimulatory capacity of the exosomes released by hyperthermia treated cancer cells. This observation is in line with previous reports that exosomes have the potential to actively affect the polarization of immune cells (Zheng, He et al. 2019). A recent study investigating murine colon adenocarcinoma- and human malignant ascite- derived exosomes has shown that an effective anti-tumor cytotoxic cascade ensued from an IL-6-dependent T cell differentiation, whereby hyperthermia-based exosomes stimulated the secretion of IL-6 from dendritic cells which belong to the mononuclear phagocyte system as macrophages (Guo, Chen et al. 2018). Interleukin-10 (IL-10), which regulates the switch of macrophages from M1 to M2 phenotype, was unchanged (Figure 7), while TNF-α was increased. However, long term tracking of the period of polarization and switching from one subset to another by using M1/M2 markers was not pursued in this study.

Regulated on Activation, Normal T Cell Expressed and Secreted (RANTES) is an inflammatory chemokine released by macrophages, which acts as a chemoattractant

for T cells (Arango Duque and Descoteaux 2014). RANTES is also known to be immunostimulatory for T cells (Lillard, Boyaka et al. 2001) and may lead to enhanced recruitment of T cells. In this study, macrophages, which became stimulated due to treatment with exosomes released by hyperthermia-treated cancer cells, also released more RANTES (Figure 7). The instance of exosomal Hsp70 eliciting a pro-inflammatory response in macrophages has been demonstrated previously but in the context of bacterial infections (Neyrolles, Anand et al. 2010). The increased immunogenic potential of exosomes secreted by cancer cells post-hyperthermia suggests potential role in hyperthermia-based cancer immunotherapies. Keeping in mind the immunogenic anti-chemotherapeutic potential of hyperthermia-based exosomes, numerous recent studies are focusing on studying the differential expression of exosomal lipids or proteins (Kelleher, Balu-Iyer et al. 2015, Shenoy, Loyall et al. 2018). Probing these hyperthermia-induced antitumorigenic immunostimulatory molecules is pertinent to accomplish a comprehensive understanding of alternative therapies like hyperthermia.

The treatement regimens used here involve hyperthermia, which can potentially induce changes in heat shock proteins. Previous studies have reported that Hsp70 or gp96 stimulate both human and murine macrophages to induce the expression of inducible nitric oxide (NO) synthase (iNOS), leading to the consequent production of NO (Panjwani, Popova et al. 2002, Song, Zhou et al. 2013), which is a characteristics marker of the M1 polarization in macrophages (Ley 2017). For these reasons, we tested the downstream effect of exosomes released by hyperthermia treated cancer cells on the polarization of RAW 264.7 macrophages and BMDMs. Polarization changes were examined by studying the changes at the transcript level of a selection of typical markers of M1 and M2 phenotypes, iNOS, and arginase-1 (Arg-1) (Ley 2017), respectively. For the transcript level study, BMDMs were included since they represent primary cells possessing the biological properties of mature macrophages and are widely accepted as a monocyte or macrophage model. Quantitative RT-PCR of the transcripts of iNOS and Arg-1, which play an essential role in regulating macrophagic pro- or anti-inflammatory response (Ley 2017), were measured in macrophages after exposure to exosomes obtained from control cells or cells exposed to hyperthermia, or LPS, which typically polarizes macrophages towards the M1 phenotype (Orecchioni, Ghosheh et al. 2019).

The iNOS is a crucial enzyme regulating macrophage inflammatory response, while Arg1 is a negative regulator of M1-mediated polarization. The transcript of iNOS was significantly upregulated in macrophages treated with exosomes obtained from 4T1 and EMT-6 cells exposed to hyperthermia, similar to LPS treatment [Figure 8, 9 (b, c)]. The Arg-1 transcript was unchanged in cells treated with LPS or exosomes obtained from EMT-6 cells exposed to hyperthermia, in comparison to cells treated with control exosomes [Figure 8 (a), 9 (a)]. However, in macrophages treated with exosomes derived from hyperthermia-treated 4T1 cells, the Arg1 transcript was also positively expressed, which may suggest that exosomes derived from 4T1 cells exposed to hyperthermia may promote a mixed M1 and M2 macrophage polarization [Figure 8 (b), 9 (a)]. This finding is in line with previous *in vitro* studies involving RAW 264.7 macrophages, where melanoma based exosomes led to a mixed phenotype (Bardi, Smith et al. 2018). Moreover, even though for our study long term tracking of the period of polarization and switching from one subset to another by using

M1/M2 markers was not pursued, it has been reported that polarization is also influenced by treatment time (Zhang, Zhang et al. 2019).

4. Discussion

Traditional chemotherapeutics have associated limitations, which include drug efflux related development of resistance and toxic side effects on non-target tissue. The failure of classical chemotherapeutics necessitates the exploration and mechanistic understanding of alternative therapeutic approaches like hyperthermia. The present study reports the immunogenic potential of hyperthermia against breast cancer at the *in vitro* level. High-temperature ranges (> 60°C) are tissue ablative, which limits their direct application in case of deep-seated tumors. Moreover, it has been reported that mild hyperthermia treatment induces immunogenic cell death (Adkins et al., 2017), which prompted our efforts to be focused on the mild hyperthermic temperature range.

In the present study, the inhibitory effect of different temperature regimens and treatment times was determined to obtain an equivalent thermal dose across the murine breast cancer cell lines EMT-6 and 4T1 and macrophagic cell line RAW 264.7. The 4T1 cells are a model of triple-negative breast cancer (TNBC), and 4T1 based tumors in BALB/c mice serve as an animal model for stage IV human breast cancer. The tumor growth dynamics, as well as the metastatic spread profile of 4T1 cells in BALB/c mice, closely mimics human breast cancer (Ouzounova, Lee et al. 2017). The EMT-6 also exhibit the characteristics of human TNBC subtype and yields non-invasive murine tumors (Ouzounova, Lee et al. 2017). Thus to investigate the response of macrophages to cues released by cancer cells after hyperthermia exposure, the metastatic (4T1) and less invasive (EMT-6) murine mammary cell lines were the cell lines of choice.

Obtaining the experimental isothermal doses across the different cell lines was pertinent for maintaining equivalent dosing effects at a given temperature. In order to determine the experimental isothermal doses across the different cell lines chosen *in vitro* viability was tested using MTT assay, which yielded convertible thermal exposure times across different temperatures. Even though 4T1 is a more aggressive cell, it was the most sensitive to mild hyperthermic exposure with respect to EMT-6 and the macrophagic cell. Since non-ablative or mild hyperthermia has gained importance as a therapeutic regimen of choice due to its potential to sensitize against radio- and chemo-therapeutics as well as induce an immunogenic response, we chose 43°C temperature point for all our subsequent experiments. The data obtained by MTT viability assay for 43°C TD_{50} corroborated with that obtained by flow cytofluorimetric analysis of viable cells.

When comparisons were made between exosomes isolated from control and hyperthermia treated experimental groups of 4T1 and EMT-6 cells under identical seeding and isolation conditions an increase in mean diameter of the exosomes in the hyperthermia treated groups was observed consistently across replicates, suggesting an increase in mean diameter due to thermal stress which may be due to enhanced packing of stress based molecular cues. The control group released homogenously sized exosomes with a greater predominance of small-sized exosomes (ExoS) while after hyperthermia treatment, larger heterogeneous sized

exosomes (ExoL) were secreted which may be attributed to release of stress-related cues. There have been several studies that show that there is an increased exosome secretion during different types of intracellular stress (Lehmann, Paine et al. 2008, Zhang, Liu et al. 2012, Kanemoto, Nitani et al. 2016, O'Neill, Gilligan et al. 2019).

In order to probe the immunogenicity of the exosomes released after hyperthermia treatment, we studied the cytokines, activation markers and morphology of macrophages exposed to hyperthermia derived exosomes. We concluded that exosomes released from cells under hyperthermic conditions, affected the functionality of the macrophages. A pronounced cytoskeletal rearrangement and increased migratory potential was observed in macrophages exposed to exosomes derived from cells exposed to hyperthermic conditions. Based on the expression of macrophage activation markers and cytokine output in RAW 264.7 cells and primary BMDM cells, we can conclude that hyperthermia based exosomes released from the breast cancer lines 4T1 and EMT-6 can elicit macrophage activation. The activation of macrophages along with an increased migratory potential observed here accompanied by the release of critical molecular cues (TNF-α or RANTES), may elicit a cytotoxic cascade against breast cancer cells. Hence, the present study indicated the potential of hyperthermia based exosomes as an active immunogenic agent with significantly increased benefits and potential to be an essential addition to the growing arsenal of immunogenic anti-chemotherapeutics.

5. Conclusions

The present study describes the assessment of the cytotoxic or inhibitory effect of different temperature regimens and treatment times to determine an equivalent thermal dose across murine breast cancer cell lines EMT-6 and 4T1 and naïve murine macrophage cell line RAW 264.7. *In vitro* analysis of the effect of different thermal doses for therapeutic applications yielded increased sensitivity of 4T1 and RAW 264.7 cells to heat, as compared to EMT-6, suggesting that hyperthermia may be an attractive treatment modality since 4T1 is known to be more aggressive and metastatic in comparison to EMT-6 (H Heppner, R Miller et al. 2000, Tao, Fang et al. 2008, Simões, Serganova et al. 2015). This insight may be of clinical value while designing treatment regimens for metastatic and aggressive tumors. Moreover, it has been reported that in lung, pancreatic, and colorectal cancer, hyperthermia increases the sensitivity of the tumor to classical chemotherapeutics (Adachi, Kokura et al. 2009, Okayama, Kokura et al. 2009, Vertrees, Das et al. 2014, Kirui, Celia et al. 2015, Cesna, Sukovas et al. 2018), highlighting the importance of designing combinatorial treatment strategies utilizing classical chemotherapeutics with hyperthermia as an adjuvant therapy.

On probing the interaction between exosomes released by breast cancer cells post-hyperthermia treatment and macrophages, it was found that exosomes released by hyperthermia treated cancer cells led to macrophage activation, cytoskeletal rearrangement, and increased migratory potential. The underlying mechanism for this enhanced immunogenic activity of the hyperthermia based exosomes could be attributed to altered size and content of the exosomes released by hyperthermia treated cancer cells, including increased Hsp-70 content. The increased migration of the macrophages upon exposure to exosomes generated by cancer cells under hyperthermic conditions accompanied by the

release of critical chemokines such as TNF-α or RANTES, may in turn alter adaptive immune response. Hence, the present study suggests the potential of exosomes released by hyperthermia-treated cancer cells treated as an immunogenic agent.

Supplementary Material

Refer to Web version on PubMed Central for supplementary material.

Acknowledgments:

This work was supported by a pilot research grant from the UF Health Cancer Center and NIH award R03AI135610. KS sincerely acknowledges Prof. Blanka Sharma and her research staff at the J. Crayton Pruitt Family Department of Biomedical Engineering at the University of Florida for providing instrument access and for their support. The authors acknowledge Prof. Kyle D. Allen of the J. Crayton Pruitt Family Department of Biomedical Engineering at the University of Florida for providing access to their incubator, which was used for all the hyperthermia experiments. The authors gratefully acknowledge Prof. Dietmar W. Siemann of the Department of Radiation Oncology, College of Medicine, University of Florida, and his research staff for providing the murine breast cancer cell lines. The authors are grateful to Prof. Russell T. Hepple and his group in the Department of Physical Therapy at the University of Florida for providing instrument support. The authors acknowledge Mark Ou of the Department of Microbiology and Cell Science, University of Florida for helping perform a replicate of the western blot. KS sincerely acknowledges fellow laboratory visiting research scholars Prof. Ivanise Guilherme Branco and Nathanne Cristina Vilela Rost for their support and encouragement.

References:

Adachi S, et al. (2009). "Effect of hyperthermia combined with gemcitabine on apoptotic cell death in cultured human pancreatic cancer cell lines." International Journal of Hyperthermia 25(3): 210–219. [PubMed: 19437237]

Amend SR, et al. (2016). "Murine Hind Limb Long Bone Dissection and Bone Marrow Isolation." Journal of Visualized Experiments(110).

Arango Duque G and Descoteaux A (2014). "Macrophage Cytokines: Involvement in Immunity and Infectious Diseases." Frontiers in Immunology 5.

Baixauli F, et al. (2014). "Exosomes and Autophagy: Coordinated Mechanisms for the Maintenance of Cellular Fitness." Frontiers in Immunology 5.

Bardi GT, et al. (2018). "Melanoma exosomes promote mixed M1 and M2 macrophage polarization." Cytokine 105: 63–72. [PubMed: 29459345]

Beninson LA and Fleshner M (2014). "Exosomes: An emerging factor in stress-induced immunomodulation." Seminars in Immunology 26(5): 394–401. [PubMed: 24405946]

Bettaieb A, et al. (2013). "Hyperthermia: Cancer Treatment and Beyond."

Cesna V, et al. (2018). "Narrow line between benefit and harm: Additivity of hyperthermia to cisplatin cytotoxicity in different gastrointestinal cancer cells." World Journal of Gastroenterology 24(10): 1072–1083. [PubMed: 29563752]

Chen T, et al. (2011). "Chemokine-Containing Exosomes Are Released from Heat-Stressed Tumor Cells via Lipid Raft-Dependent Pathway and Act as Efficient Tumor Vaccine." The Journal of Immunology 186(4): 2219–2228. [PubMed: 21242526]

de Jong OG, et al. (2012). "Cellular stress conditions are reflected in the protein and RNA content of endothelial cell-derived exosomes." Journal of Extracellular Vesicles 1(1): 18396.

De Toro J, et al. (2015). "Emerging Roles of Exosomes in Normal and Pathological Conditions: New Insights for Diagnosis and Therapeutic Applications." Frontiers in Immunology 6.

Desdín-Micó G and Mittelbrunn M (2016). "Role of exosomes in the protection of cellular homeostasis." Cell Adhesion & Migration 11(2): 127–134. [PubMed: 27875097]

Ghazaei C (2017). "Role and mechanism of the Hsp70 molecular chaperone machines in bacterial pathogens." Journal of Medical Microbiology 66(3): 259–265. [PubMed: 28086078]

Gonzalez-Angulo AM, et al. (2007). "Overview of resistance to systemic therapy in patients with breast cancer." Breast Cancer Chemosensitivity 608: 1–22.

Guo D, et al. (2018). "Exosomes from heat-stressed tumour cells inhibit tumour growth by converting regulatory T cells to Th17 cells via IL-6." Immunology 154(1): 132–143. [PubMed: 29197065]

H Heppner G, et al. (2000). "Nontransgenic models of breast cancer." Breast Cancer Research 2(5).

Ha PT, et al. (2019). "Doxorubicin release by magnetic inductive heating and in vivo hyperthermia-chemotherapy combined cancer treatment of multifunctional magnetic nanoparticles." New Journal of Chemistry 43(14): 5404–5413.

Han C, et al. (2019). "Human umbilical cord mesenchymal stem cell derived exosomes encapsulated in functional peptide hydrogels promote cardiac repair." Biomaterials Science.

Hessvik NP and Llorente A (2017). "Current knowledge on exosome biogenesis and release." Cellular and Molecular Life Sciences 75(2): 193–208. [PubMed: 28733901]

Hui WW, et al. (2018). "Salmonella enterica Serovar Typhimurium Alters the Extracellular Proteome of Macrophages and Leads to the Production of Proinflammatory Exosomes." Infect Immun 86(2).

Hui WW, et al. (2018). "Salmonella enterica Serovar Typhimurium Alters the Extracellular Proteome of Macrophages and Leads to the Production of Proinflammatory Exosomes." Infection and Immunity 86(2).

Ito A, et al. (2003). "Heat shock protein 70 gene therapy combined with hyperthermia using magnetic nanoparticles." Cancer Gene Therapy 10(12): 918–925. [PubMed: 14712318]

Ito A, et al. (2001). "Augmentation of MHC class I antigen presentation via heat shock protein expression by hyperthermia." Cancer Immunol Immunother 50(10): 515–522. [PubMed: 11776373]

Jeong S (2014). "The Combination of Hyperthermia, Radiation, and Chemotherapy for Tumor Suppression Using Hollow Gold Nanoparticles." International Journal of Radiation Oncology*Biology*Physics 90(1): S804.

Kanemoto S, et al. (2016). "Multivesicular body formation enhancement and exosome release during endoplasmic reticulum stress." Biochemical and Biophysical Research Communications 480(2): 166–172. [PubMed: 27725157]

Kelleher RJ, et al. (2015). "Extracellular Vesicles Present in Human Ovarian Tumor Microenvironments Induce a Phosphatidylserine-Dependent Arrest in the T-cell Signaling Cascade." Cancer Immunology Research 3(11): 1269–1278. [PubMed: 26112921]

Kirui DK, et al. (2015). "Mild Hyperthermia Enhances Transport of Liposomal Gemcitabine and Improves In Vivo Therapeutic Response." Advanced Healthcare Materials 4(7): 1092–1103. [PubMed: 25721343]

Krakhmal NV, et al. (2015). "Cancer Invasion: Patterns and Mechanisms." Acta Naturae 7(2): 17–28. [PubMed: 26085941]

Lehmann BD, et al. (2008). "Senescence-Associated Exosome Release from Human Prostate Cancer Cells." Cancer Research 68(19): 7864–7871. [PubMed: 18829542]

Ley K (2014). "The second touch hypothesis: T cell activation, homing and polarization." F1000Research 3: 37. [PubMed: 25580220]

Ley K (2017). "M1 Means Kill; M2 Means Heal." The Journal of Immunology 199(7): 2191–2193. [PubMed: 28923980]

Lillard JW, et al. (2001). "RANTES Potentiates Antigen-Specific Mucosal Immune Responses." The Journal of Immunology 166(1): 162–169. [PubMed: 11123289]

Mathieu M, et al. (2019). "Specificities of secretion and uptake of exosomes and other extracellular vesicles for cell-to-cell communication." Nature Cell Biology 21(1): 9–17. [PubMed: 30602770]

Moreno-Aspitia A and Perez EA (2009). "Treatment options for breast cancer resistant to anthracycline and taxane." Mayo Clin Proc 84(6): 533–545. [PubMed: 19483170]

Mummidi S, et al. (2013). "Macrophage Migration and Invasion Is Regulated by MMP10 Expression." PLoS ONE 8(5): e63555. [PubMed: 23691065]

Neyrolles O, et al. (2010). "Exosomal Hsp70 Induces a Pro-Inflammatory Response to Foreign Particles Including Mycobacteria." PLoS ONE 5(4): e10136. [PubMed: 20405033]

O'Neill C, et al. (2019). "Role of Extracellular Vesicles (EVs) in Cell Stress Response and Resistance to Cancer Therapy." Cancers 11(2): 136.

Okayama T, et al. (2009). "Antitumor effect of pretreatment for colon cancer cells with hyperthermia plus geranylgeranylacetone in experimental metastasis models and a subcutaneous tumor model of colon cancer in mice." International Journal of Hyperthermia 25(2): 141–149. [PubMed: 19337914]

Orecchioni M, et al. (2019). "Macrophage Polarization: Different Gene Signatures in M1(LPS+) vs. Classically and M2(LPS−) vs. Alternatively Activated Macrophages." Frontiers in Immunology 10.

Ouzounova M, et al. (2017). "Monocytic and granulocytic myeloid derived suppressor cells differentially regulate spatiotemporal tumour plasticity during metastatic cascade." Nature Communications 8(1).

Panjwani NN, et al. (2002). "Heat Shock Proteins gp96 and hsp70 Activate the Release of Nitric Oxide by APCs." The Journal of Immunology 168(6): 2997–3003. [PubMed: 11884472]

Phung DC, et al. (2019). "Combined hyperthermia and chemotherapy as a synergistic anticancer treatment." Journal of Pharmaceutical Investigation.

Poh AR and Ernst M (2018). "Targeting Macrophages in Cancer: From Bench to Bedside." Frontiers in Oncology 8.

Pozzi LAM, et al. (2005). "Both Dendritic Cells and Macrophages Can Stimulate Naive CD8 T Cells In Vivo to Proliferate, Develop Effector Function, and Differentiate into Memory Cells." The Journal of Immunology 175(4): 2071–2081. [PubMed: 16081773]

Ratajczak J, et al. (2006). "Membrane-derived microvesicles: important and underappreciated mediators of cell-to-cell communication." Leukemia 20: 1487. [PubMed: 16791265]

Rezaie J, et al. (2017). "Exosomes and their Application in Biomedical Field: Difficulties and Advantages." Molecular Neurobiology 55(4): 3372–3393. [PubMed: 28497202]

Roberts DD, et al. (2018). "Evaluation of phenotypic and functional stability of RAW 264.7 cell line through serial passages." PLoS ONE 13(6): e0198943. [PubMed: 29889899]

Sapareto SA and Dewey WC (1984). "Thermal dose determination in cancer therapy." Int J Radiat Oncol Biol Phys 10(6): 787–800. [PubMed: 6547421]

Seifert G, et al. (2016). "Regional hyperthermia combined with chemotherapy in paediatric, adolescent and young adult patients: current and future perspectives." Radiation Oncology 11(1).

Selli C and Sims AH (2019). "Neoadjuvant Therapy for Breast Cancer as a Model for Translational Research." Breast Cancer: Basic and Clinical Research 13: 117822341982907.

Sen K, et al. (2019). "Dual drug loaded liposome bearing apigenin and 5-Fluorouracil for synergistic therapeutic efficacy in colorectal cancer." Colloids and Surfaces B: Biointerfaces 180: 9–22. [PubMed: 31015105]

Shao Q, et al. (2019). "Engineering T cell response to cancer antigens by choice of focal therapeutic conditions." International Journal of Hyperthermia 36(1): 130–138. [PubMed: 30676126]

Sharma S, et al. (2018). "Ascent of atomic force microscopy as a nanoanalytical tool for exosomes and other extracellular vesicles." Nanotechnology 29(13): 132001. [PubMed: 29376505]

Shenoy GN, et al. (2018). "Exosomes Associated with Human Ovarian Tumors Harbor a Reversible Checkpoint of T-cell Responses." Cancer Immunology Research 6(2): 236–247. [PubMed: 29301753]

Sheppe AEF, et al. (2018). "PGE2 Augments Inflammasome Activation and M1 Polarization in Macrophages Infected With Salmonella Typhimurium and Yersinia enterocolitica." Front Microbiol 9: 2447. [PubMed: 30429830]

Siegel RL, et al. (2019). "Cancer statistics, 2019." CA: A Cancer Journal for Clinicians 69(1): 7–34. [PubMed: 30620402]

Simões RV, et al. (2015). "Metabolic Plasticity of Metastatic Breast Cancer Cells: Adaptation to Changes in the Microenvironment." Neoplasia 17(8): 671–684. [PubMed: 26408259]

Skitzki JJ, et al. (2009). "Hyperthermia as an immunotherapy strategy for cancer." Curr Opin Investig Drugs 10(6): 550–558.

Song S, et al. (2013). "PDT-induced HSP70 externalization up-regulates NO production via TLR2 signal pathway in macrophages." FEBS Letters 587(2): 128–135. [PubMed: 23247210]

Tao K, et al. (2008). "Imagable 4T1 model for the study of late stage breast cancer." BMC Cancer 8(1).

Théry C, et al. (2006). "Isolation and Characterization of Exosomes from Cell Culture Supernatants and Biological Fluids." Current Protocols in Cell Biology 30(1): 3.22.21–23.22.29.

Toraya-Brown S and Fiering S (2014). "Local tumour hyperthermia as immunotherapy for metastatic cancer." International Journal of Hyperthermia 30(8): 531–539. [PubMed: 25430985]

van Rhoon GC (2016). "Is CEM43 still a relevant thermal dose parameter for hyperthermia treatment monitoring?" International Journal of Hyperthermia 32(1): 50–62. [PubMed: 26758036]

van Rhoon GC, et al. (2013). "CEM43°C thermal dose thresholds: a potential guide for magnetic resonance radiofrequency exposure levels?" European Radiology 23(8): 2215–2227. [PubMed: 23553588]

Vertrees RA, et al. (2014). "Synergistic interaction of hyperthermia and gemcitabine in lung cancer." Cancer Biology & Therapy 4(10): 1144–1153.

Vulpis E, et al. (2019). "Cancer Exosomes as Conveyors of Stress-Induced Molecules: New Players in the Modulation of NK Cell Response." International Journal of Molecular Sciences 20(3): 611.

Williams EC, et al. (2019). "Precious cargo." Journal of Trauma and Acute Care Surgery 86(1): 52–61.

Wu J, et al. (2013). "Nitric Oxide and Interleukins are Involved in Cell Proliferation of RAW264.7 Macrophages Activated by Viili Exopolysaccharides." Inflammation 36(4): 954–961. [PubMed: 23515856]

Yagawa Y, et al. (2017). "Cancer immunity and therapy using hyperthermia with immunotherapy, radiotherapy, chemotherapy, and surgery." Journal of Cancer Metastasis and Treatment 3(10): 218.

Zhang H-C, et al. (2012). "Microvesicles Derived from Human Umbilical Cord Mesenchymal Stem Cells Stimulated by Hypoxia Promote Angiogenesis Both In Vitro and In Vivo." Stem Cells and Development 21(18): 3289–3297. [PubMed: 22839741]

Zhang H, et al. (2018). "Identification of distinct nanoparticles and subsets of extracellular vesicles by asymmetric flow field-flow fractionation." Nature Cell Biology 20(3): 332–343. [PubMed: 29459780]

Zhang W, et al. (2019). "Lipopolysaccharide mediates time-dependent macrophage M1/M2 polarization through the Tim-3/Galectin-9 signalling pathway." Experimental Cell Research 376(2): 124–132. [PubMed: 30763585]

Zhang Y, et al. (2019). "Exosomes: biogenesis, biologic function and clinical potential." Cell & Bioscience 9(1).

Zheng Y, et al. (2019). "Exosomes from LPS-stimulated macrophages induce neuroprotection and functional improvement after ischemic stroke by modulating microglial polarization." Biomaterials Science 7(5): 2037–2049. [PubMed: 30843911]

Zhou X, et al. (2017). "Characterization of mouse serum exosomal small RNA content: The origins and their roles in modulating inflammatory response." Oncotarget 8(26).

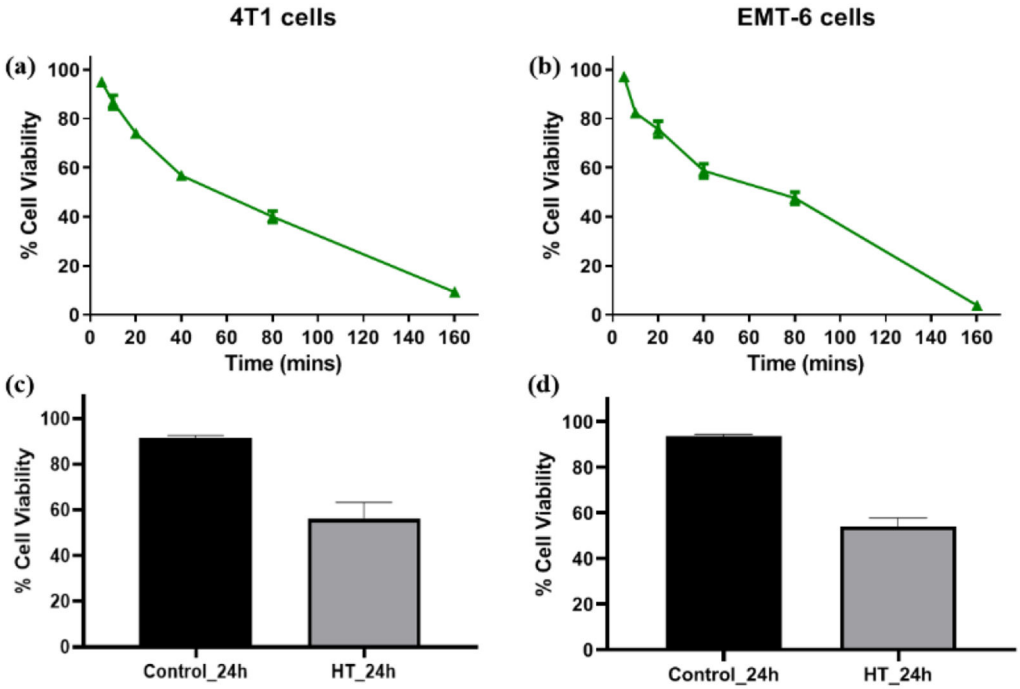

Figure 1.

(a, b) Cell viability of 4T1 and EMT-6 cells after treatment at 43° C determined using MTT assay. The cell viability of untreated cells was considered as 100%. **(c, d)** Cell viability of 4T1 and EMT-6 using Annexin V-FITC-PI-based FACS at CEM43 TD_{50} [Individual replicate data provided in supplementary materials Figure S-3].

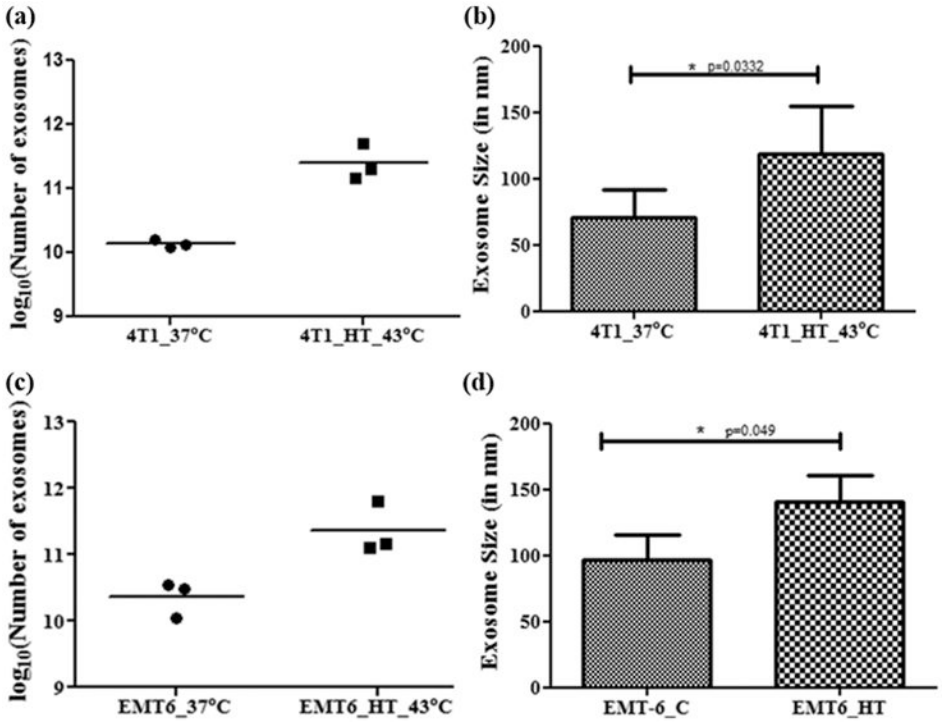

Figure 2:

NTA analysis of isolates of 4T1 and EMT-6 derived exosomes. **(a, c)** Data represents the number of exosomes obtained from isolation replicates (n = 3, p=0.0376 for 4T1, p=0.0174 for EMT-6). The exosome yield reported here has been standardized to exosomes per 10^7 viable cells at the time of exosome isolation. **(b, d)** Data represents the average size distribution profile from isolation replicates (n = 3). Student's t-test was used for comparing data between the two groups. [Individual replicate data provided in supplementary materials Figure S-4, S-5].

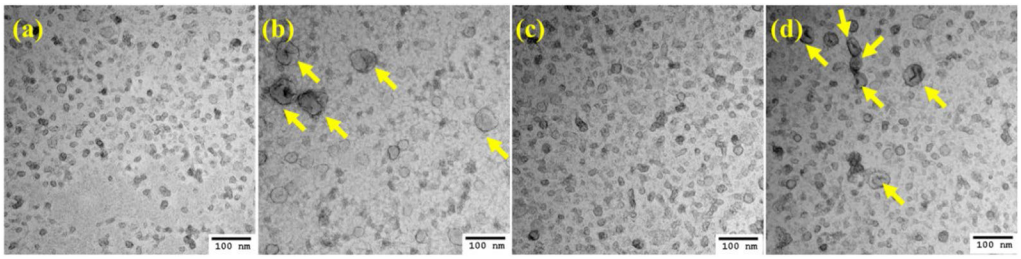

Figure 3.

TEM images of negatively stained exosomes. **(a)** 4T1 control exosomes, **(b)** 4T1 exosomes post-hyperthermia treatment, **(c)** EMT-6 control exosomes, and **(d)** EMT-6 exosomes post-hyperthermia treatment. Yellow arrows signify the presence of relatively larger exosomes observed in greater abundance in hyperthermia-based treated sets.

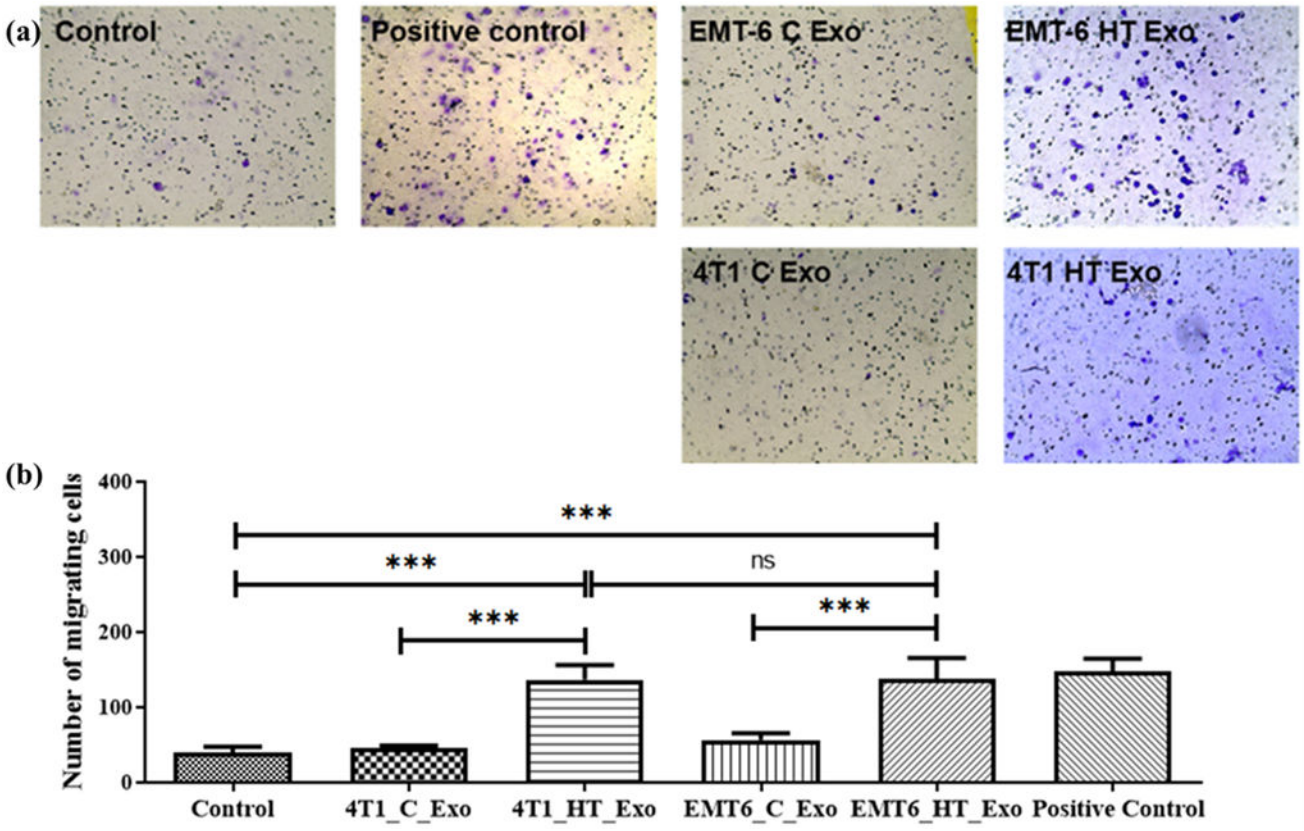

Figure 4.

(a) Bright-field images of transwell migration of RAW 264.7 cells upon treatment with LPS (positive control), EMT-6 control exosomes, EMT-6 exosomes post-hyperthermia treatment, 4T1 control exosomes, and 4T1 exosomes post-hyperthermia treatment. **(b)** Transwell migratory profile of RAW 264.7 macrophages upon treatment with LPS (positive control), EMT-6 control exosomes, EMT-6 exosomes post-hyperthermia treatment, 4T1 control exosomes, and 4T1 exosomes post-hyperthermia treatment. Each bar represents the mean ± standard error (n=3). One-way ANOVA followed by Tukey's test was used for comparing data between groups, where *** indicates $p < 0.001$ between bracketed groups.

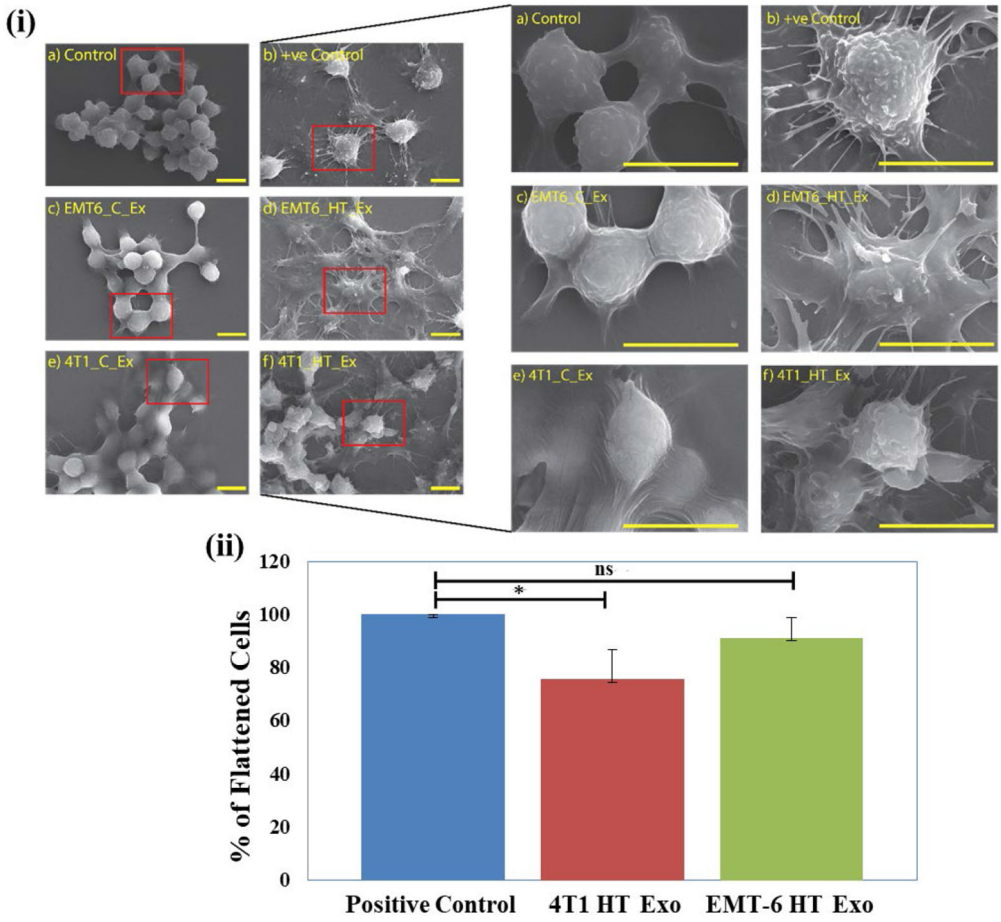

Figure 5.

(i) SEM images of **(a)** Untreated negative control, **(b)** Positive control (LPS-treated), **(c, e)** control exosome-treated and **(d, f)** hyperthermia derived exosome treated RAW 264.7 cells (scale bar represents 10 μm), **(ii)** Percentage of flattened cells in positive control, post-hyperthermia derived exosome treated RAW 264.7 cells compared to respective controls after 24 hours treatment. Each bar represents the mean ± standard deviation with sample size (number of counted cells) >50. The student's t-test was used for comparing data between the two groups (n=3), where * indicates $p < 0.05$.

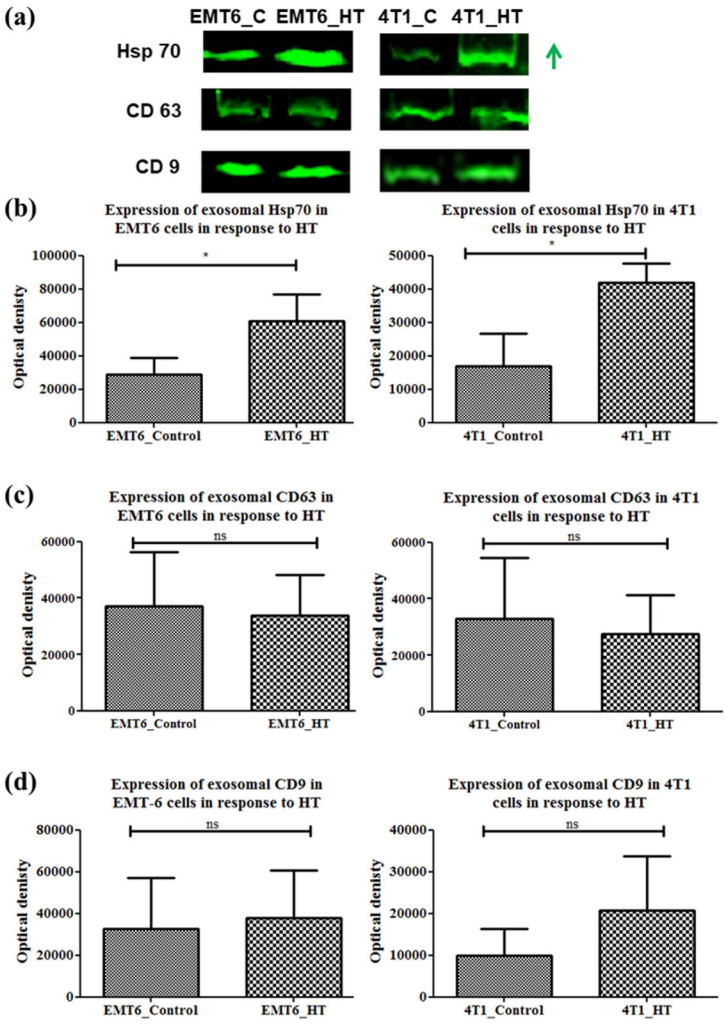

Figure 6.

Western blot analysis of Hsp70, CD9, CD63 proteins in exosomes from control untreated or hyperthermia treated EMT-6 and 4T1 cells with individual densitometry analysis. Each bar represents the mean optical density ± standard error (n=3). The student's t-test was used for comparing data between the two groups (n=3), where * indicates $p < 0.05$. The green arrow in **(a)** represents increased expression (signal intensity).

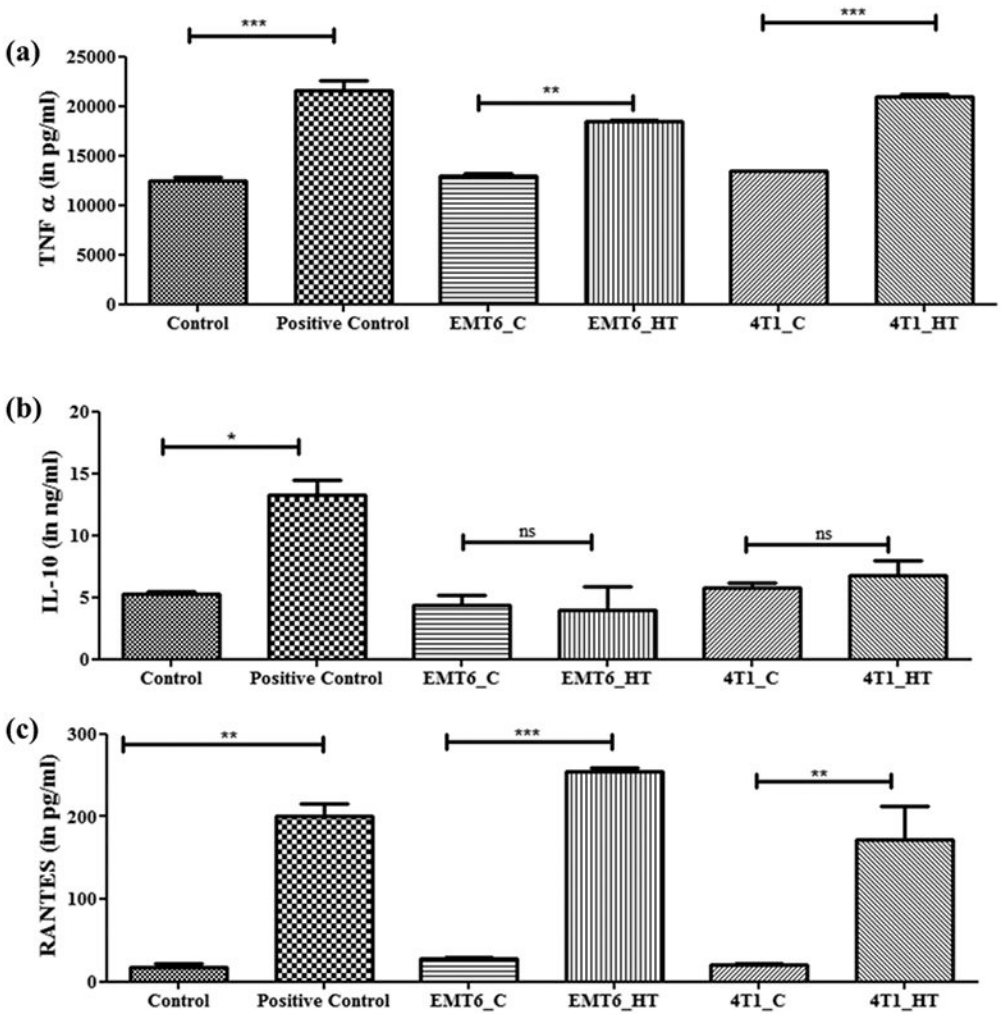

Figure 7.

Untreated or hyperthermia based exosome-mediated alterations in inflammatory or downstream signaling pathways as observed in RAW 264.7 macrophages. Each bar represents the mean concentration ± standard error (n=3). One-way ANOVA followed by Tukey's test was used for comparing data between groups, where * indicates $p < 0.05$, ** indicates $p < 0.01$, and *** indicates $p < 0.001$ between bracketed groups.

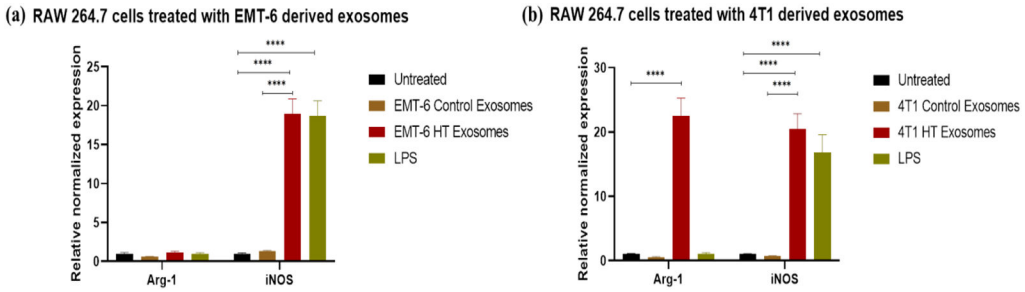

Figure 8.

qRT-PCR profile of macrophage polarization marker expression (normalized to GAPDH) in RAW 264.7 after 24 hours exposure to control and hyperthermia based exosomes from 4T1 and EMT-6 cells, respectively. One-way ANOVA followed by Tukey's test was used for comparing data between groups, where * indicates $p < 0.05$, ** indicates $p < 0.01$, and *** indicates $p < 0.001$ between bracketed groups (n=3).

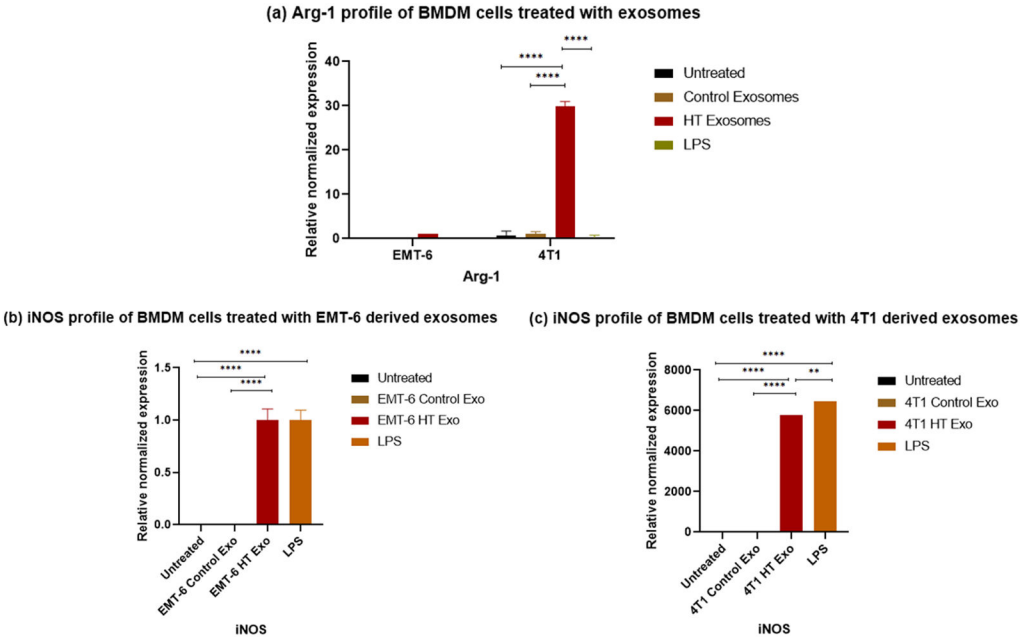

Figure 9.

qRT-PCR profile of macrophage polarization marker expression (normalized to GAPDH) in BMDMs following the exposure to control exosomes or exosomes derived from 4T1 and EMT-6 cells exposed to hyperthermia. **(a)** Arg-1 profile of BMDM cells following 24 hours exposure to control and hyperthermia based exosomes from 4T1 and EMT-6 cells respectively, **(b-c)** iNOS profile of BMDM cells after 24 hours exposure to control exosomes or exosomes derived from 4T1 and EMT-6 cells exposed to hyperthermia. The Arg-1 and iNOS expression level in untreated control and EMT-6 control exosomes treated BMDM cells in **(a,b)** is close to zero and hence not visible in the graph. Similarly iNOS expression level is negligible in untreated control and 4T1 control exosome treated BMDM cells in **(c)** and hence not visible in the graph. One-way ANOVA followed by Tukey's test was used for comparing data between groups, where * indicates $p < 0.05$, ** indicates $p < 0.01$ and *** indicates $p < 0.001$ between bracketed groups (n=3).

Table 1.

Primers used for the detection of transcripts.

Gene name/Oligo	Sequence
GAPDH Forward Mouse	ACTCCACTCACGGCAAAATTC
GAPDH Reverse Mouse	CCAGTAGACTCCACGACATACT
iNOS Forward Mouse	GGTGAAGGGACTGAGCTGTT
iNOS Reverse Mouse	ACGTTCTCCGTTCTCTTGCAG
Arg-1 Forward Mouse	TTTTAGGGTTACGGCCGGTG
Arg-1 Reverse Mouse	CCTCGAGGCTGTCCTTTTGA

Table 2.

Thermal Dose$_{50}$ (TD$_{50}$) for EMT-6, 4T1, and RAW 264.7 cells after treatment at different temperatures and their CEM43 Thermal Dose$_{50}$ (CEM TD$_{50}$) equivalents.

Temperature / Cell line	45°C		44°C		43°C	
	TD$_{50}$	CEM TD$_{50}$	TD$_{50}$	CEM TD$_{50}$	TD$_{50}$	CEM TD$_{50}$
4T1	9.1±1.4min	36.4±5.6min	23.5±1.5min	47±3min	42.8±1.5min	42.8±1.5min
EMT-6	20.0±1.6min	80±6.4min	34.4±0.13min	68.7±0.26min	81.7±0.24min	81.7±0.24min
RAW 264.7	14±3.4min	56±13.6min	23.3±1.92min	46.6+3.84min	50.3±2min	50.3±2min

Table 3:

Exosome size in EMT-6 or 4T1 derived control and hyperthermia treated sets.

Experimental Set	Exosome Size and Characteristics		
	Replicate 1	**Replicate 2**	**Replicate 3**
4T1 Control	55.2±8.5 nm	94.7±26.7 nm	65.3±5.7 nm
	Single Peak	Dominant Peak with Several Smaller Peaks	Single Peak
4T1 HT_43°C	95.3±39.5 nm	100.1±51.6 nm	160.4±81.5 nm
	Multiple Peaks	Multiple Peaks	Multiple Peaks
EMT-6 Control	76±16.4 nm	100.8±32 nm	113.2±15.9 nm
	Single Peak	Single Peak	Dominant Peak with a Smaller Peak
EMT-6 HT_43°C	128.8±15.9 nm	164.1±82.4 nm	127.9±63.8 nm
	Multiple Peaks	Multiple Peaks	Multiple Peaks